SLAC–PUB–7617
October 1997
(A)

Experiments on the Fast Beam-Ion Instability at the ALS*

F. Zimmermann*, J. Byrd†, A. Chao*, S. Heifets*, M. Minty*,
T. Raubenheimer‡, J. Seeman*, G. Stupakov*, J. Thomson†

*Stanford Linear Accelerator Center, Stanford, California 94309
†Lawrence Berkeley National Laboratory, Berkeley, California 94720
‡CERN, PS Division, CH-1211, Geneva 23, Switzerland

We report on the first observation of the fast beam–ion instability (FBII), at the Advanced Light Source (ALS). The FBII is a novel single-pass instability, which is similar to the classical beam break up instability in a linac. Unlike the classical trapped-ion instability, the FBII cannot be cured by a clearing gap in the bunch train, and it is predicted to be a potential limitation for many multi-bunch small-emittance storage rings and linacs. In order to induce the FBII in the ALS, we added helium gas to the vacuum system so as to increase the vacuum pressure by two orders of magnitude above its normal value. At an elevated pressure of about 50–100 nTorr, we observed a variety of effects, including an increase of the vertical beam size by a factor 2–4, self-excited betatron sidebands, and a growth of the betatron motion along the bunch train. The onset of the vertical beam-size increase (as a function of bunch number) occured close to the theoretically predicted instability threshold.

Invited Talk at the International Workshop on Multi-Bunch Instabilities in Future Electron and Positron Accelerators (MBI97), KEK, Tsukuba, Japan, July 15–18, 1997

*Work supported by the U.S. Department of Energy under Contract Nos. DE-AC03-76SF00098 and DE-AC03-76SF00515 and by the Tsukuba EXPO'85 Memorial Foundation.

Experiments on the Fast Beam-Ion Instability at the ALS*

F. Zimmermann*, J. Byrd†, A. Chao*, S. Heifets*, M. Minty*,
T. Raubenheimer‡, J. Seeman*, G. Stupakov*, J. Thomson†

*Stanford Linear Accelerator Center, Stanford, California 94309
†Lawrence Berkeley National Laboratory, Berkeley, California 94720
‡CERN, PS Division, CH-1211, Geneva 23, Switzerland

Abstract

We report on the first observation of the fast beam–ion instability (FBII), at the Advanced Light Source (ALS). The FBII [1, 2] is a novel single-pass instability, which is similar to the classical beam break up instability in a linac. Unlike the classical trapped-ion instability, the FBII cannot be cured by a clearing gap in the bunch train, and it is predicted to be a potential limitation for many multi-bunch small-emittance storage rings and linacs. In order to induce the FBII in the ALS, we added helium gas to the vacuum system so as to increase the vacuum pressure by two orders of magnitude above its normal value. At an elevated pressure of about 50–100 nTorr, we observed a variety of effects, including an increase of the vertical beam size by a factor 2–4, self-excited betatron sidebands, and a growth of the betatron motion along the bunch train. The onset of the vertical beam-size increase (as a function of bunch number) occured close to the theoretically predicted instability threshold.

1 INTRODUCTION

When a charged particle beam passes through an accelerator beam pipe, ions are generated in the residual gas. These ions have long been recognized as a potential limitation in electron and antiproton storage rings, where they may cause large tune shifts or transverse instabilities [7, 8, 9, 10] and lifetime reductions. Such classical ion effects are induced by ions which are accumulated over many turns and trapped by the electric field of the beam. Often, the ions can be removed by intentionally introducing a gap in the bunch train, in which the ions are overfocused and lost to the chamber wall. For example, the design of the PEP-II B factory at SLAC includes a gap of 352 ns (5% of the ring circumference), during whose passage most of the ions generated by the 1658-bunch train will disappear. As a consequence, classical multi-turn ion effects are not expected to be important for PEP-II.

However, if a beam consists of a train of many bunches with small transverse emittances, effects of single-pass ions may become significant. These are ions which are generated during a single passage of the bunch train, and whose density increases roughly linearly along the train. In the gap at the end of the train the ions are lost, and there is only an insignificant number of ions left when the train returns on its next revolution. As a numerical example, in the PEP-II High Energy Ring the ion line density at the end of the bunch train is about 10^6 m^{-1}, assuming an average pressure of 5 nTorr and carbon monoxide molecules.

A schematic of the FBII is shown in Fig. 1 (top picture). If there is a small initial perturbation in the relative transverse bunch positions along the train, the ions produced by a leading bunch are offset with respect to some trailing bunch. The latter is then deflected by the electric field of the ion cloud produced by the former. This mechanism can lead to an instability where the oscillation amplitude increases exponentially along the bunch train. This is quite reminiscent of the classical beam break-up in a linac. To distinguish this instability from conventional multi-turn ion instabilities, it has been called the 'fast beam-ion instability' (FBII). Since it is a single-pass effect, the fast beam-ion instability can occur in either storage rings or linacs. The same type of instability is also predicted for a single positron bunch (see the bottom picture of Fig. 1). In this case the atomic electrons, generated by the gas ionization, oscillate within the positron bunch in quite the same manner as the ions would oscillate within the electron bunch train. The electrons are lost in the gap between positron bunches, similar to the ion loss at the end of the electron bunch train. For otherwise identical parameters, the rise-time estimates for the single-bunch positron instability are usually much larger than those for the multi-bunch ion-electron instability, primarily because a single bunch generates much fewer ions (or electrons) than an entire train.

To experimentally confirm the predicted instability for an electron bunch train, in 1996 we performed a series of experiments at the Advanced Light Source, in which the vacuum pressure was artificially raised to 50–100 nTorr by a remotely controlled inflow of helium gas. We thus established conditions where the fast beam-ion instability was expected to occur. In this report, we describe the results of our experiments. The experimental set up and preliminary results have already been discussed in Refs. [5, 6].

In the following section, we summarize the theoretical predictions for the fast beam-ion instability, and we list estimated instability rise times for many existing or proposed accelerators. Section 3 introduces the Advanced Light Source and the diagnostics used in the FBII studies. The experimental results are discussed in Section 4. Finally, in Section 5. we give a summary and draw some conclusions, and we present plans for future ion-instability

* This work was supported by the U.S. Department of Energy under Contract Nos. DE-AC03-76SF00098 and DE-AC03-76SF00515 and by the Tsukuba EXPO'85 Memorial Foundation.

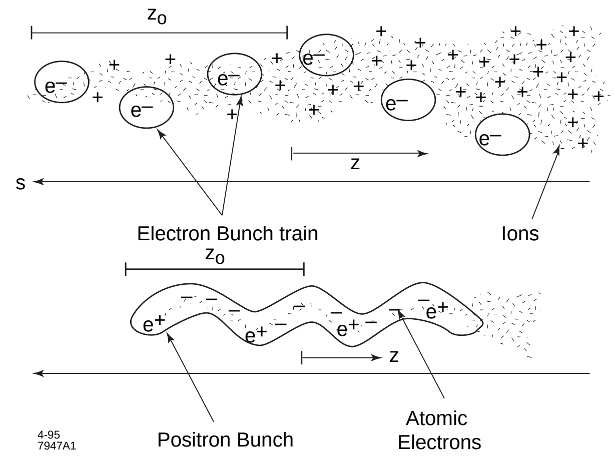

Figure 1: Schematic of the fast beam-ion instability, which can arise either due to ion trapping within an electron bunch train or due to trapping of free electrons for the case of a positron bunch.

studies at the ALS.

2 THEORY AND RISE-TIME PREDICTIONS

The FBII growth rate strongly depends on the number of bunches, the transverse beam sizes, and the residual-gas pressure. Analytical expressions for the growth rate at the end of the bunch train have been derived using three different approximations [1, 2, 3, 4]. In a simple linear treatment, which is applicable for small amplitudes ($y \ll \sigma_y$), an initial vertical perturbation of magnitude $\hat{y}$ is found to increase quasi-exponentially as [1]

$$y \approx \hat{y}\, \frac{1}{2\sqrt{2\pi}(t/\tau_c)^{1/4}}\ \exp(\sqrt{t/\tau_c}) \qquad (1)$$

with a characteristic time

$$\frac{1}{\tau_c} \equiv \frac{4 d_{gas}\sigma_{ion}\beta N_b^{3/2} n_b^2 r_e r_p^{1/2} L_{sep}^{1/2} c}{\sqrt{3}\,3\gamma\sigma_y^{3/2}(\sigma_x+\sigma_y)^{3/2}A^{1/2}}. \qquad (2)$$

Here, $d_{gas} = p/(kT)$ denotes the residual gas density (where p is the gas pressure, k Boltzmann's constant, and T the absolute temperature), β the average vertical beta function, N_b the bunch population, n_B the number of bunches in the train, L_{sep} the bunch spacing (in meters), σ_x and σ_y the horizontal and vertical beam size, respectively, γ the beam energy in units of the rest energy, A the ion mass as a multiple of the proton mass, r_e ($\approx 2.8\times10^{-15}$ m) the classical electron radius, r_p ($\approx 1.5\times10^{-18}$ m) the classical proton radius, c the speed of light, and σ_{ion} the cross section for collisional ionization. The ionization cross section σ_{ion} for nitrogen or carbon monoxide is about 2 Mbarn; the cross section for helium or hydrogen is about 10 times smaller, with a correspondingly reduced growth rate.

If the ion decoherence—caused, for example, by the dependence of the vertical ion oscillation frequency on the horizontal position—and the variation of the ion frequency along the beam line are included in the analytical derivation, Eq. (1) is replaced by a purely exponential growth [2, 3]

$$y \sim \exp(t/\tau_e) \qquad (3)$$

with an e-folding time of

$$\frac{1}{\tau_e} \approx \frac{1}{\tau_c}\,\frac{c}{4\sqrt{2}\pi L_{sep} n_b a_{bt} f_i}, \qquad (4)$$

where

$$f_i \equiv \frac{c}{\pi}\left(\frac{Q N_b r_p}{3 A L_{sep}\sigma_y(\sigma_x+\sigma_y)}\right)^{\frac{1}{2}} \qquad (5)$$

denotes the coherent ion oscillation frequency, and $2a_{bt}$ the peak-to-peak ion-frequency variation ($a_{bt} \approx 0.1$–1; the smaller number applies to a FODO cell and the larger to a typical light-source optics, *e.g.*, to a Chasman-Green cell.) Also Eq. (3) is only valid for amplitudes small compared with the beam size.

Computer simulations indicate that the instability growth rate dramatically slows down at amplitudes of about 2–5 σ_y, where the beam-ion force becomes very nonlinear. The nonlinear force also leads to a filamentation in phase space, resulting in a larger beam size and a correspondingly further reduced growth rate.

Disregarding any such filamentation effects and using a simplified analytical model, Heifets showed that for very large oscillation amplitudes ($y \gg \sigma_y$), a linear growth is expected [4], *i.e.*,

$$y \sim \sigma_y\,\frac{t}{\tau_H} \qquad (6)$$

with a time constant

$$\frac{1}{\tau_H} \approx \frac{1}{\tau_c}\,\frac{c}{2\pi f_i L_{sep} n_b^{3/2}} \qquad (7)$$

According to Eq. (6) at large amplitudes the oscillation amplitude grows only linearly as a function of time, so that, in reality, the growth will eventually be balanced by some exponential damping mechanism, *e.g.*, by a transverse multibunch feedback system or by synchrotron radiation. An analytical estimate of the equilibrium beam size in the presence of noise excitation and feedback was recently derived by Chao and Stupakov [12].

The FBII arises only when the ions are trapped between bunches. The trapping condition can approximately be written as

$$4 L_{sep} f_i / c \leq 1 \qquad (8)$$

In an experiment, the number of single-pass ions could be inferred from the tune shift that the ions induce along the bunch train. At the end of the bunch train the ion-induced incoherent tune shift is given by

$$\Delta Q_y = \frac{r_e \beta_y \lambda_{ion} C}{\gamma 2\pi\sigma_y(\sigma_x+\sigma_y)} \qquad (9)$$

where β_y denotes the average vertical beta function, C the ring circumference, and λ_{ion} the ion line density at the end of the train. The coherent tune shift along the train is about two thirds of the incoherent tune shift.

It is interesting to notice that for a constant average current, the three alternative formulae for the instability rise time, Eqs. (1), (4), and (6), predict a very different dependence on the number of bunches [11]:

$$\tau_c \propto \sqrt{n_b} \qquad (10)$$

$$\tau_e \propto 1 \qquad (11)$$

$$\tau_H \propto 1/\sqrt{n_b} \qquad (12)$$

This difference could be used to determine experimentally the applicability of the various theories!

In Table 1 we list parameters and predicted instability rise times for three accelerators related to a next-generation linear collider, namely for the proposed damping ring and the main linac of the Next Linear Collider [13] and for the prototype damping ring ATF which is presently being commissioned at KEK. The projected rise times are exceedingly short: in all cases the characteristic time τ_c is of the order of a few hundred nanoseconds or less, the e-folding time τ_e is a few microseconds and even τ_H is much smaller than a millisecond. These rise times are unprecedentedly small. Table 1 suggests that the ATF damping ring provides the unique opportunity to study collective single-pass ion effects in a parameter regime which is very similar to (actually, even more severe than) that expected for a next linear collider.

accelerator	NLC e− DR	NLC ML	ATF DR
ϵ_x^N [μm]	3	3	4.3
ϵ_y^N [nm]	30	30	30
n_b	90	90	20
N_b [10^{10}]	1.5	1.5	2
$\beta_{x,y}$ [m]	2	8	2.5
σ_x [μm]	40	35	83
σ_y [μm]	4	3.5	5
L_{sep} [cm]	42	42	84
C [m]	223	—	139
E [GeV]	2	10	1.54
p [nTorr]*	1	10	60
f_i [MHz] †	176	201	90
$4L_{sep}f_i/c$	0.98	1.12	1.02
ΔQ_y [10^{-3}]	2.5	—	18
τ_c [ns]	500	42	187
τ_e [μs]	20	1.9	1.6
τ_H [μs]	660	64	27

Table 1: Parameters and predicted oscillation growth rates for the NLC electron damping ring [13], the first section of the NLC main linac [13], and the ATF damping ring (presently being commisioned) [14, 15];
*partial pressure of carbon monoxide or nitrogen;
†assuming carbon monoxide as a typical species.

In Table 2 we present, for comparison, an equivalent list of nominal parameters for 4 operating accelerators: the ALS at LBNL, the ESRF in Grenoble, the HERA electron ring at DESY, and CESR at Cornell. The calculated instability rise times are considerably larger than those of Table 1. The characteristic time τ_c now varies between 1 μs and a few 100 μs, the e-folding time is a few ms, and the linear rise time at large amplitudes, τ_H, is even longer. The predicted instability rise time τ_e for the ALS is ten times larger than the damping time of the transverse multibunch feedback system, and thus the fast beam-ion instability should not be observed during routine operation. The same is true for the HERA electron ring, where the feedback damping time is of the order of 0.1 ms, 50 times shorter than the estimated instability rise time. Also in CESR, the instability rise time is quite modest, comparable to the head-tail or radiation damping times (which are about 5 ms and 20 ms, respectively [16]). We note that, using Eq. (8), in CESR the ions are not stably trapped between bunches, which will lead to a reduction of the instability growth rate.

Table 2 indicates that from all the storage rings in routine operation, the ESRF appears to be the only one in which the fast beam-ion instability might be observed under nominal operating conditions. Since the ESRF uses a Chasman-Green lattice, with a large variation of the ion oscillation frequency around the ring, the theoretical prediction for the ESRF is more uncertain than that for a regular FODO cell lattice, for which $\beta_x(s) \times \beta_y(s) \approx$ constant (the uncertainty enters in the form of the parameter a_{bt} in Eq. (4)). We were not able to gather much information about the composition of the residual gas in the ESRF. If we suppose that 95% of the residual gas is hydrogen, whose ions are too light to be trapped in the bunch train, the partial carbon monoxide pressure would only be 0.1 nTorr, and the instability rise time $\tau_e \approx 6$ ms would be comparable to the radiation damping time ($\tau_y \approx 7$ ms). Experimental observations with regard to the ESRF are not well documented; according to some informal reports [17] vertical instabilities are indeed observed, but it has not been determined if these are caused by ions or if they are normal coupled-bunch instabilities. In practice, the instabilities are suppressed by introducing a large positive chromaticity [17]. Whether the observed instabilities are caused by ions or not, head-tail damping (due to the large chromaticity) should also damp the FBII.

In order to create experimental conditions where the fast beam-ion instability should definitely occur, we raised the vacuum pressure in the Advanced Light Source to about 80 nTorr. At this pressure, the predicted rise time exceeds the feedback damping time by a significant factor. The vacuum system was vented with helium gas, since, for helium, the expected rms emittance growth due to beam-gas scattering is small (a few percent at 100 nTorr). Table 3 compares the ALS parameters chosen for our experiments with those anticipated for the PEP-II High Energy Ring. According to all three rise time estimates—τ_c, τ_e and τ_H—, the instability in the ALS experiment is faster than that predicted for PEP-II.

accelerator	ALS	ESRF	HERA e−	CESR
ϵ_x^N [μm]	12	73	2000	2700
ϵ_y^N [μm]	0.2	0.7	110	120
n_b	320	300	210	7
N_b [10^{10}]	0.7	1	3.7	46
$\beta_{x,y}$ [m]	2.5, 4	4,12	25	14, 13
σ_x [μm]	101	213	1000	2000
σ_y [μm]	17	11	230	400
L_{sep} [m]	0.60	1	29	96
C [m]	200	844	6300	670
E [GeV]	1.5	6	26	5
p [nTorr]*	1	2	1	5
f_i [MHz]†	20	25	0.85	0.87
$4L_{sep}f_i/c$	0.155	0.33	0.31	1.11
ΔQ_y [10^{-3}]	0.1	6	0.26	0.04
τ_c [μs]	18	0.7	170	1000
τ_e [ms]	4	0.3	4.9	3.5
τ_H [ms]	25	2	250	33

Table 2: Parameters and oscillation growth rates for some existing accelerators: the Advanced Light Source, the European Synchrotron Radiation Facility [18], the HERA electron ring (presently being operated with positrons), and CESR;
*the measured pressure is taken to be equal to the partial pressure of carbon monoxide (depending on the actual gas composition, this could overestimate the growth rate by up to a factor 10–20);
†assuming carbon-monoxide molecules.

accelerator	ALS experiment	PEP-II HER
ϵ_x^N [μm]	12	500
ϵ_y^N [μm]	0.4	25
n_b	160, **240**, 320	1658
N_b [10^{10}]	0.4–0.8	3
$\beta_{x,y}$ [m]	2.5, 4	25, 20
σ_x [μm]	200	1250
σ_y [μm]	20	200
L_{sep} [m]	0.6	1.2
E [GeV]	1.5	9
p [nTorr]	80‡	5*
f_i [MHz]	40‡	4*
$4L_{sep}f_i/c$	0.34	0.15
ΔQ_y [10^{-3}]	3.2	6.1
τ_c [μs]	0.4	2
τ_e [μs]	14–140	74–740
τ_H [ms]	0.76	10.7

Table 3: Parameters and predicted oscillation growth rates for the ALS machine experiment compared with those for the PEP-II High-Energy Ring.
‡for helium atoms; *assuming carbon-monoxide or nitrogen molecules.

3 THE ADVANCED LIGHT SOURCE

The Advanced Light Source (ALS) is a 3rd generation light source, operating at 1.5 GeV and optimized for producing high brightness synchrotron radiation. Table 4 lists the nominal machine parameters.

The ALS is currently operating for users at the design current of 400 mA. So far 5 insertion devices have been installed and 12 light beamlines are operational. Under normal operating conditions (with 320 bunches), feedback systems are used to control the conventional transverse and longitudinal coupled-bunch instabilities.

parameter	description	value
E	beam energy	1.5 GeV
C	circumference	196.8 m
f_{rf}	RF frequency	499.654 MHz
σ_ϵ	RMS $\delta E/E$	7.1e-4
h	harmonic number	328
σ_x	av. hor. beam size	100 μm
σ_y	av. vert. beam size	17 μm
ϵ_x	norm. hor. emittance	1.2×10^{-5} m
ϵ_y	norm. vert. emittance	4×10^{-7} m
α	momentum compaction	1.594e-3
Q_s	synchrotron tune	0.0075
σ_ℓ	RMS natural bunch length	4.5 mm
$Q_{x,y}$	betatron tunes (x,y)	14.28, 8.18

Table 4: Nominal ALS parameters.

3.1 Transverse Coupled-Bunch Feedback System

During our studies, the ALS transverse coupled–bunch feedback (TFB) systems [21, 22] played an important rôle. For multibunch beam currents above ∼50 mA, the beam in the ALS executes large amplitude coupled–bunch oscillations in both the horizontal and vertical directions. Previous studies have correlated the beam oscillations with known RF cavity higher-order modes and with the resistive wall impedance [20]. For all data presented in the next section, the vertical, horizontal, and longitudinal FB systems were active. In the following, our hypothesis is that during our experiment the coupled bunch oscillations were successfully damped by the feedback system while the ion-induced oscillations were not damped during their initial growth.

As input signal to the TFB, the transverse moments of the bunch $I\Delta x, I\Delta y$ are detected at two points in the ring, with nominal betatron phase differences (modulo 2π) of approximately 65 and 245 degrees in the x, y directions. The TFB receivers are implemented as heterodyne detectors centered at 3 GHz ($6\times f_{rf}$) with a bandpass of ±250 MHz. The 3-GHz was chosen as the local oscillator frequency, because it is near the frequency of maximum impedance of the button pickups. We used a monitor of the baseband signal from one of the receivers as a diagnostic of coherent centroid oscillations in the control room.

A diagram of the TFB systems is shown in Fig. 2. Two features of the TFB are relevant to our studies. First, the sensitivity of the heterodyne receivers to vertical oscillations is less than a micron, significantly smaller than the average vertical beam sizes. Second, the damping rate of

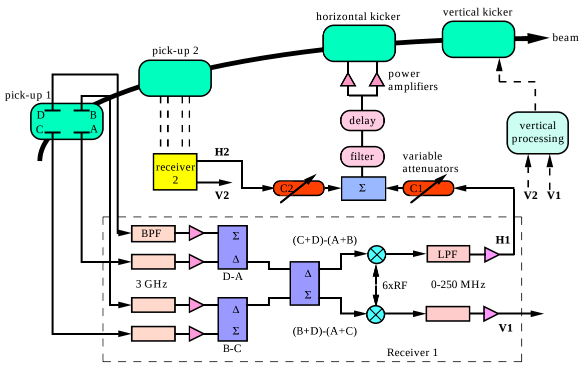

Figure 2: ALS transverse feedback systems.

the TFB is linearly dependent on the bunch current and also somewhat sensitive to the system phase adjustments, making it difficult to predict the precise damping rate of the system without a direct measurement (the feedback damping time can be determined either from the oscillation decay time after excitation with an injection kicker magnet, or from the evolution of unstable modes after the feedback has been switched off temporarily [20]). For the conditions in the experiments presented below, the damping time of the vertical FB system is about 0.3–0.4 msec at 1 mA/bunch although this was not measured at the time of the experiments.

3.2 Synchrotron Light Image

Our main diagnostic was an image of the transverse beam profile at one location of the storage ring using light from synchrotron radiation [19]. The photon optics consist of grazing incidence mirrors with an optical magnification of unity. A carbon foil eliminates light with $\lambda\ >5$ nm, for which the image of the vertical beam size would be diffraction-limited. The transmitted soft x-rays are converted to visible light using a scintillator and then focused onto a CCD camera. Unfortunately the response time of the scintillator is long—300 ns, about half the revolution period—, so that it does not allow beam-size measurements of individual bunches within the bunch train.

3.3 Transverse Beam Spectrum

Another diagnostic in the experiment was the spectrum of transverse dipole beam oscillations. We observed the beam spectrum in the control room using an HP70000 spectrum analyzer. Computer control of the analyzer allowed automatic recording of the amplitudes of all 328 betatron sidebands from 0 to 250 MHz. Most of the data in the high pressure regime were taken with a Tektronix 3052 spectrum analyzer, which uses 1024 parallel digital signal processors to quickly produce a Fourier transform of the input signal. We used this in combination with the HP70000 spectrum analyzer in the following way. The 321.4 MHz IF signal from the spectrum analyzer was down-converted to 7.5 MHz using a Tektronix 162 downconverter and input to the TEK3052. Using the fast processing of the TEK3052 the time required to scan all of the betatron sidebands was less than 10 minutes. As an example, Fig. 3 shows the spontaneous (*i.e.*, self-excited) vertical upper and lower betatron sidebands near the 4th and 5th rotation harmonics.

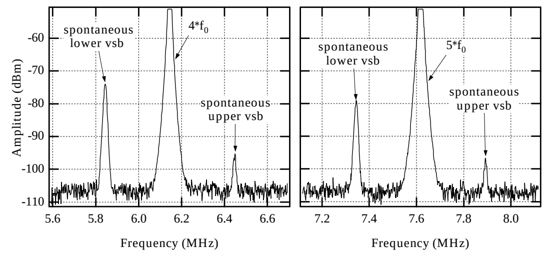

Figure 3: Raw spectrum of vertical pickup shown near the 4th and 5th revolution harmonics.

3.4 ALS Vacuum System

For UHV operation, the vacuum in the ALS is pumped by a combination of passive titanium sublimation pumps which are distributed throughout the ring and 107 active noble diode ion pumps. The pressure is detected using 12 ion gauges and from the currents in the ion pumps. The ion gauges are calibrated to read the equivalent pressure for diatomic nitrogen. For normal operation of the ring, the average pressure with beam is about 0.25 nTorr. For the FBII experiment, we installed a small gas inlet in the ring that could be used to bleed in helium gas so as to maintain a consistent high gas pressure.

To reach the high pressure it was necessary to turn off all of the ion pumps except for a pump on either side of the RF cavities, which are located adjacent to one another in one of the ring's twelve straight sections. The gas inlet ports are located on either side of these pumps in order to balance the gas distribution throughout the ring. By adjusting the gas inlet rate, we could maintain an average pressure of $\sim$80 nTorr of helium around the ring as measured using the ion gauges. Residual gas analyzers indicated that helium was the dominant gas species by an order of magnitude. Hydrogen and argon were the next most populous species. Following the completion of a high pressure experiment, the noble diode ion pumps were turned on and the vacuum recovered in 10–15 minutes. To date, we have not been able to measure the effect on the beam of other helium pressures. We are currently exploring the feasibility of adding other gas species.

4 EXPERIMENT

We bled in an appropriate amount of helium to maintain the desired high gas pressure. The motivation for using helium gas is that the vertical emittance growth from Coulomb scattering is only a few percent effect and that calculations indicated an achievable level of helium pressure (<100

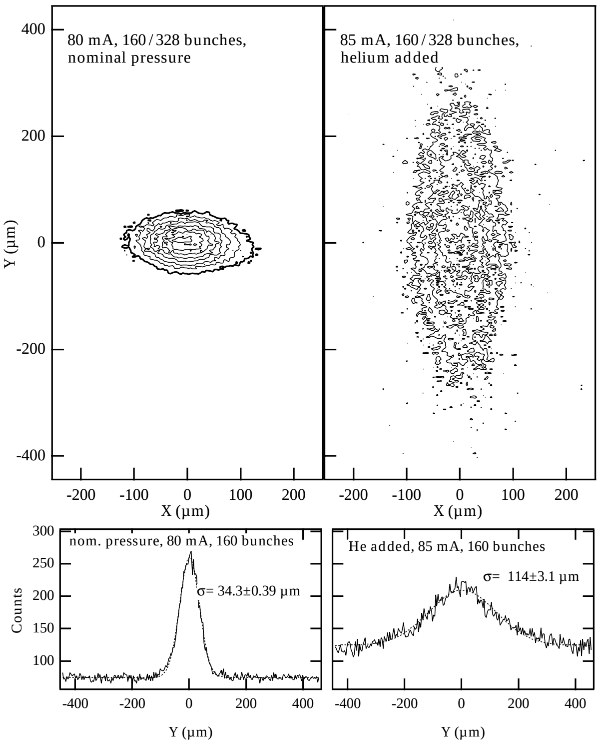

Figure 4: Transverse profile images (shown as contour plots) of the beam for nominal pressure and with helium added; the vertical profile for each image is also shown along with a fit to a gaussian distribution.

nTorr) would give an FBII growth rate much faster than the damping rate of the TFB system. We recall that our goal was to create a condition where the coupled-bunch oscillations driven by the ring impedance would be stabilized by the TFB system but oscillations driven by the FBII would be unstable, thereby allowing us to distinguish between the two effects.

The experimental procedure was to record the synchrotron light image and the vertical beam spectrum for bunch patterns with 240, 200 and 160 consecutive buckets filled (roughly 3/4, 5/8 and 1/2 of the ring) at both the nominal and the elevated pressure. We also recorded the beam image of a single bunch, and found that the single-bunch beam size increase with pressure (by a few percent) agreed well with the expected emittance growth due to beam-gas scattering.

Shown in Figure 4 are transverse beam profiles from the synchrotron light monitor measured for the case of 160 successive bunches at the nominal pressure (left) and at an elevated helium pressure of about 80 nTorr (right). At the higher pressure, the vertical beam size dramatically increased while the horizontal beam size was unchanged. Underneath each image is a vertical profile of the image, fitted to a Gaussian distribution with the rms value shown.

We studied the onset of the instability by recording the beam behavior as the length of the bunch train was slowly increased. Starting with a single bunch of 0.5 mA, we

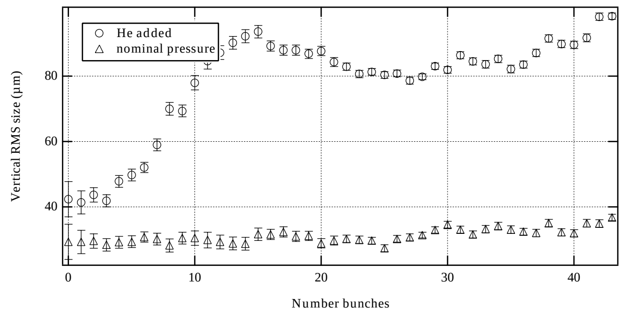

Figure 5: RMS vertical beam size versus the number of bunches for nominal and elevated pressure conditions.

slowly filled consecutive bunches. Shown in Figure 5 is a plot of the RMS vertical beam size (average over all bunches stored) as a function of the number of bunches continuing up to a total of 45 bunches. Also shown are the corresponding vertical beam sizes at nominal pressure. With helium gas added, the beam size increased significantly at a threshold corresponding to about 8 bunches. The predicted growth rates τ_c and τ_e for the 8th bunch under these conditions are about $(1\ \mathrm{ms})^{-1}$. Thus they are approximately equal to the feedback damping rate for a current of 0.5 mA/bunch. In other words, the observed instability threshold at a train length of about 8 bunches agrees quantitatively with the theoretical prediction!

The vertical beam spectrum for several different cases is shown in Figure 6. For simplicity, we have plotted the difference between the lower and upper sidebands. (The FBII theory predicts that only the lower sideband is unstable). A positive value indicates a larger lower sideband. The coherent vertical sidebands were not present at the nominal pressure. As helium was added, a pattern of lower sidebands appeared with a peak amplitude at a frequency near that predicted by FBII simulations. For increasing beam current, the coherent signal shifted upwards in frequency as expected. A comparison of the coherent oscillation frequencies from experiments and theory is shown in Figure 7.

In addition, when we enlarged the vertical beam size by operating very close to the linear coupling resonance, we observed that the coherent signal shifted downwards in frequency. Such a frequency shift is expected for the FBII, since the ion oscillation frequency in Eq. (5) depends on the vertical beam size. This is in stark contrast to conventional coupled-bunch instabilities, for which the frequency of an unstable mode should not depend on the beam size.

It should also be mentioned that we did not observe a coherent signal for all cases even though we always observed a vertical beam-size increase when helium was added. The exact reason for this is not yet understood. One possible explanation is that for large growth rates the coherent vertical oscillations filament very rapidly, only persisting in the form of an enhanced vertical size. We hope to resolve this question in subsequent experiments.

Although we did not have the instrumentation for mea-

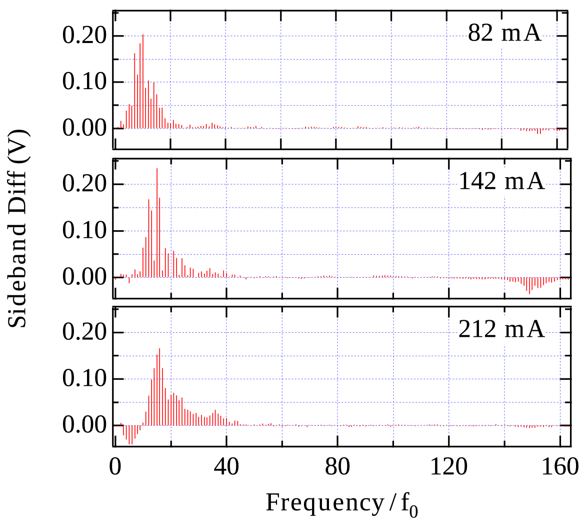

Figure 6: Vertical betatron sidebands measured in the 240/328 fill pattern for three different currents. The frequency axis is scaled by the revolution frequency.

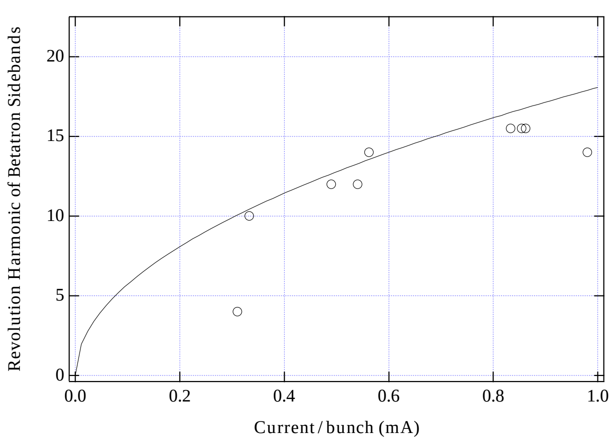

Figure 7: Comparison between the measured and predicted frequency of coherent beam oscillations for 240/320 fill pattern.

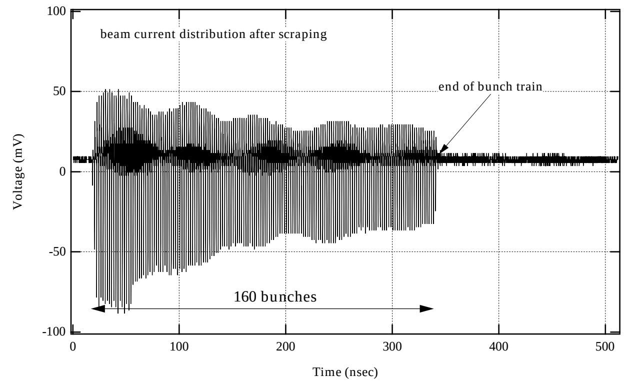

Figure 8: Beam current along the bunch train for 160 bunches after moving a vertical aperture close to the beam. The nonuniform loss pattern shows the increasing vertical oscillations (or beam size) along the bunch train.

suring the vertical oscillations of each bunch in the train, we were able to measure the relative oscillation amplitudes or the relative beam sizes by moving a vertical aperture (i.e. scraper) close to the beam and detecting the current loss along the bunch train. The signal from a beam position monitor, in Fig. 8, shows the relative current along the bunch train after scraping the beam. Starting from a uniform current distribution, the scraper reduced the bunch population in the tail about 2.5 times more than that of the leading bunches, indicating that either the oscillation amplitude or the beam size (or both) increased along the train. The nonuniform loss pattern proves the transient nature of the instability, which is one of the main predictions of the FBII theory.

5 CONCLUSIONS

5.1 Summary

In the Advanced Light Source the fast beam-ion instability is not observed at the normal operating pressure (0.3 nTorr). When 80 nTorr helium gas was added to the vacuum, the vertical beam size increased by a factor 2–4 in a regime where multiturn ion trapping is not expected and where a single bunch only showed a marginal beam-size increase due to gas scattering. The beam loss pattern after vertical scraping shows that the tail of the bunch train was driven more strongly than the head. The instability threshold as a function of the number of bunches was observed exactly at that point where the predicted instability rise times τ_c and τ_e are equal to the feedback damping time!

Self-excited betatron sidebands, which, in our experiment, were sometimes but not always observed, peaked at a value consistent with the calculated ion oscillation frequency. The peak frequency increased with current as expected, and it decreased when the vertical beam size was increased by setting the betatron tunes close to the linear coupling resonance. Finally, the instability growth saturated at amplitudes of 2–4 σ_y, which is also predicted both by theory and simulation.

In conclusion, all observations so far appear to be in good agreement with the theoretical predictions for the fast beam-ion instability.

5.2 Future Plans

In the next ALS experiments, tentatively scheduled for the fall of 1997, we intend

- to measure the emittance blow-up for a short bunch train with the multibunch feedback system turned off and to study the effect of noise in the TFB systems (HOM-driven coupled-bunch instabilities are not thought to be a problem if there are only a few bunches in the ring, while on the other hand noise induced by the feedback which is being amplified by the FBII could be responsible for the observed blow-up),
- to investigate the effectiveness of a large chromaticity in reducing the instability growth rate,
- to determine the instability threshold for different gas pressures,
- to measure the tune shift and the oscillation amplitude of each bunch along the train, and
- to test potential cures.

One potential cure is the introduction of additional short gaps in the bunch train to clear the ions. Preliminary simulation results for the NLC damping ring [23], depicted in Fig. 9, indicate that additional gaps can be effective in slowing down the instability.

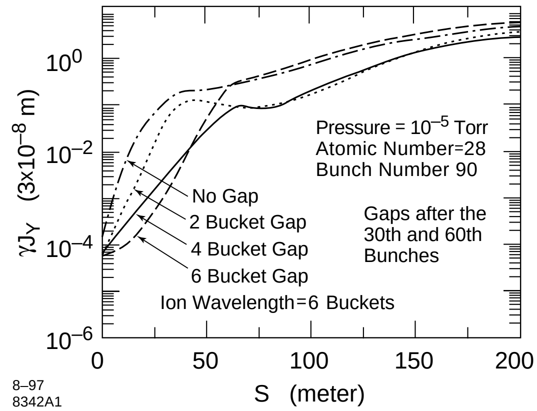

Figure 9: Effects of gaps in the bunch train on the instability growth rate in the NLC damping ring, calculated by a macroparticle simulation [1, 23]. The horizontal coordinate is the distance along the ring in meters; the vertical coordinate is the normalized action variable for the centroid of the 90th bunch in units of the rms design emittance, on a logarithmic scale. The four curves correspond to different gap sizes: 0, 2, 4 and 6 empty buckets, respectively. To reduce the computing time, the simulation was performed for a vacuum pressure of 10^{-5} Torr, which is 10^4 times higher than the nominal pressure of 1 nTorr.

6 ACKNOWLEDGEMENTS

We would like to thank Dr. A. Jackson for his support and the operations crew of the Advanced Light Source for their assistance with the machine experiments. We also thank Prof. S. Kurokawa, Dr. Y.-H. Chin and Dr. Y. Funakoshi for the invitation to the MBI97 workshop and for financial support.

7 REFERENCES

[1] T.O. Raubenheimer and F. Zimmermann, ”Fast Beam-Ion Instability I: Linear Theory and Simulations” SLAC-PUB-6740, Phys. Rev. E, Vol. 52, 5, pp. 5487–5498 (1995).

[2] G.V. Stupakov, T.O. Raubenheimer and F. Zimmermann, ”Fast Beam-Ion Instability II: Effect of Ion Decoherence”, SLAC-PUB-6805, Phys. Rev. E, Vol. 52, 5, pp. 5499–5504 (1995).

[3] G.V. Stupakov, “A Fast Beam-Ion Instability”, Proceedings of the International Workshop on Collective Effects and Impedance for B-Factories (CEIBA95), KEK Proceedings 96-6, August 1996, p. 243 (1996).

[4] S.A. Heifets, “Saturation of the ion induced transverse blow up instability”, PEP-II AP-Note No.:95-20, and Proceedings of the International Workshop on Collective Effects and Impedance for B-Factories (CEIBA95), KEK Proceedings 96-6, Aug. 1996, p. 270.

[5] J. Byrd, A. Chao, S. Heifets, M.G. Minty, T. Raubenheimer, J. Seeman, G. Stupakov, J. Thomson, F. Zimmermann, ”First observations of a 'Fast Beam-Ion Instability' ”, Physical Review Letters, Vol. 79, no. 1, p. 79, CERN-CLIC-NOTE-325, SLAC-PUB-7507 (1997).

[6] J. Byrd, A.W. Chao, S. Heifets, M.G. Minty, T. Raubenheimer, J. Seeman, G. Stupakov, J. Thomson, F. Zimmermann, ”Ion Instability Experiments on the ALS”, to be published in the Proceedings of the 12th Advanced ICFA Beam Dynamics Workshop on Nonlinear and Collective Phenomena in Beam Physics, Arcidosso, Italy, and SLAC-PUB-7389 (1996).

[7] G. Koshkarev and Zenkevich, Part. Acc. 3, “Resonance of Coupled Transverse Oscillations in Two Circular Beams”, p. 1 (1972).

[8] J.M. Laslett, A.M. Sessler, D. Möhl, “Transverse Two-Stream Instability in the Presence of Strong Species-Species and Image Forces”, Nuclear Instruments and Methods 121, p. 517–524 (1974).

[9] R. Alves Pires et al., “On the Theory of Coherent Instabilities Due to Coupling Between a Dense Cooled Beam and Charged Particles from the Residual Gas,” Proc. 1989 Part. Accel. Conf., Chicago, p. 800.

[10] D. Sagan and A. Temnykh, “Observations of the coherent beam-ion interaction in the CESR storage ring”, Nucl. Instr. and Methods A 344 p. 459 (1994).

[11] Y.H. Chin emphasized this point during the workshop.

[12] A. Chao and G. Stupakov, these proceedings (1997).

[13] Zeroth Order Design Report for the Next Linear Collider, The NLC Design Group, LBNL-5424, SLAC-474, UCRL-ID-124161, UC-414 (1996).

[14] F. Hinode et al., “ATF Design and Study Report”, KEK Internal 95–4 (1995).

[15] T.O. Raubenheimer et al., “The Vertical Emittance in the ATF Damping Ring”, Nucl. Instr. Meth. A335, p. 1 (1992).

[16] J. Rogers, private communication (1997).

[17] A. Ropert, private communication (1997).

[18] C. Limbourg, private communication to D. Brandt (1995).

[19] R. Keller, T. Renner, D. J. Massoletti, “Electron beam diagnostics using synchrotron radiation at the ALS”, Proceedings of the Seventh Beam Instrumentation Workshop (BIW96), Argonne (1996).

[20] J. Byrd, W. Barry, J. Corlett, J. Fox, D. Teytelman, “Observations of collective effects at the Advanced Light Source”, presented at the International Workshop on Collective Effects and Impedances for B–Factories, KEK, June 1995, (1996).

[21] W. Barry, J. Byrd, J. Corlett, G. Lambertson, C. C. Lo, “Transverse coupled-bunch feedback in the ALS”, Proceedings of the 1994 EPAC, July 1994.

[22] J. Byrd, W. Barry, “Controlling the vertical mode coupling instability with feedback in the Advanced Light Source”, presented at the 12th Advanced ICFA Beam Dynamics Workshop on Nonlinear and Collective Phenomena in Beam Physics, Arcidosso, Italy Sept. 2–10, 1996 (1996).

[23] T. Raubenheimer, unpublished (1996).